# Prethermal Floquet Steady States and Instabilities in the Periodically Driven, Weakly Interacting Bose-Hubbard Model

Marin Bukov,[1,*] Sarang Gopalakrishnan,[2] Michael Knap,[2,3] and Eugene Demler[2]
[1]Department of Physics, Boston University, 590 Commonwealth Avenue, Boston, Massachusetts 02215, USA
[2]Department of Physics, Harvard University, 17 Oxford Street, Cambridge, Massachusetts 02138, USA
[3]Physics Department, Walter Schottky Institute, and Institute for Advanced Study, Technical University Munich, 85748 Garching, Germany
(Received 10 July 2015; published 11 November 2015)

We explore prethermal Floquet steady states and instabilities of the weakly interacting two-dimensional Bose-Hubbard model subject to periodic driving. We develop a description of the nonequilibrium dynamics, at arbitrary drive strength and frequency, using a weak-coupling conserving approximation. We establish the regimes in which conventional (zero-momentum) and unconventional [$(\pi,\pi)$-momentum] condensates are stable on intermediate time scales. We find that condensate stability is *enhanced* by increasing the drive strength, because this decreases the bandwidth of quasiparticle excitations and thus impedes resonant absorption and heating. Our results are directly relevant to a number of current experiments with ultracold bosons.

DOI: 10.1103/PhysRevLett.115.205301 PACS numbers: 67.85.Hj, 05.45.-a, 05.60.Gg, 05.70.Ln

Periodically driven systems [1–4] often exhibit exotic phenomena that are absent in their nondriven counterparts [5–7]. Classic examples include the Kapitza pendulum and the periodically kicked rotor. Recently, periodically modulating optical lattices has attracted interest as a way of controlling hopping processes [8–14] in order to engineer gauge fields [15–22], topological band structures [23–29], and associated exotic states of matter. Such exotic states are known to exist in noninteracting systems and in certain mean-field models; the extent to which they survive in the presence of interactions is a central open question. It is believed, from the eigenstate thermalization hypothesis [30–32], that driven interacting systems will generically heat up to infinite temperature at sufficiently late times [33–40]. Nevertheless, in some parameter regimes these heating times will be parametrically slower than the system's characteristic time scales. In that case, the system will rapidly approach a "prethermalized" Floquet steady state [39,41–43], which governs the dynamics until the much later heating time scales.

In the present Letter, we study these prethermal states in the weakly interacting, two-dimensional, periodically driven Bose-Hubbard model (BHM). The regime we explore is directly relevant to experiments [10,11,14,17–19,21,22,26], in which weak interactions are present. We employ a self-consistent weak-coupling conserving approximation (WCCA) which treats the coupled nonlinear dynamics of the condensate and the quasiparticle spectrum while neglecting collisions between quasiparticles. This approximation is justified at weak coupling since nonlinearities are important at much shorter times than the collisional time scales.

Within the WCCA, we find a phase diagram (Fig. 1) featuring at low drive frequency a regime in which the superfluid state is *already* unstable within Bogoliubov theory, owing to the resonant creation of quasiparticle pairs, and a regime (at high drive frequency) where the superfluid is stable. In the WCCA, there is a sharp phase transition between these; when effects beyond weak coupling are included, there will be a qualitative difference in heating rates. Thus, in the "stable" regions of Fig. 1, the system initially reaches a prethermalized superfluid state—featuring a nonequilibrium quasiparticle distribution—and then eventually heats up. For strong driving, the prethermalized superfluid state is exotic, involving condensation at

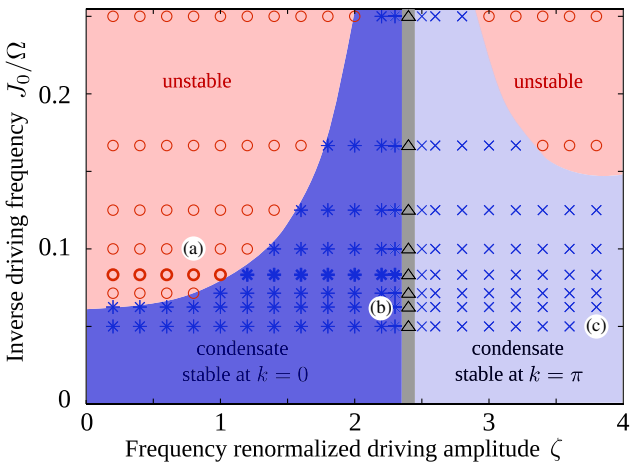


FIG. 1 (color online). Stability diagram of the driven BHM for $U/J_0 = 0.2$. In the pink regions the condensate is unstable as the drive parametrically excites pairs of quasiparticles. In contrast, in the blue regions the condensate is stable on intermediate time scales. In the grey shaded region around $\zeta \approx 2.405$ the system is strongly correlated (see text). The symbols represent numerical WCCA results; the boundaries are given by the analytical expression Eq. (5). Points marked (a), (b), (c) correspond to the panels in Fig. 3.

 

momentum $\boldsymbol{\pi} = (\pi, \pi)$. The existence of this exotic phase in the high-frequency limit has previously been established [8,9,11]; we find that it persists for intermediate frequencies as well.

Remarkably, we find that the stable phase is *enhanced* for intermediate drive strengths, since the drive both creates quasiparticle pairs when this is a resonant process and decreases the effective hopping rate (and, thus, the effective bandwidth of quasiparticle excitations). A key conclusion of our Letter is that, for weak interactions but general drive amplitude and frequency, the condensate becomes unstable when the drive frequency is parametrically resonant with the drive-renormalized time-averaged bandwidth. Therefore, parametric resonance occurs at *lower* frequencies when the drive strength is ramped up.

*Model.*—We consider the Bose-Hubbard model on a square lattice in the presence of a circularly polarized time-periodic force $\mathbf{E}(t) = A(\cos\Omega t, \sin\Omega t)^T$,

$$H_{\mathrm{lab}}(t) = -J_0 \sum_{\langle ij \rangle} b_i^\dagger b_j + \sum_j \left[ \frac{U}{2} n_j(n_j - 1) + \mathbf{E}(t) \cdot \mathbf{r}_j n_j \right]. \tag{1}$$

The operator $b_j^\dagger$ creates a boson on lattice site $\mathbf{r}_j$. The tunneling and interaction strength are denoted by $J_0$ and $U$, respectively. To achieve nontrivial dynamics in the high-frequency regime, we scale the driving amplitude linearly with the driving frequency $A \sim \Omega$ [6]; we define $\zeta \equiv A/\Omega$. We transform this Hamiltonian into a rotating frame (cf. Supplemental Material [44]), giving

$$H(t) = -J_0 \sum_{\langle ij \rangle} e^{i\mathcal{A}(t)\cdot(\mathbf{r}_i - \mathbf{r}_j)} b_i^\dagger b_j + \frac{U}{2} \sum_j n_j(n_j - 1). \tag{2}$$

Thus, in the rotating frame, the system experiences an effective time-dependent gauge potential $\mathcal{A}(t) = \zeta(\sin\Omega t, -\cos\Omega t)^T$. The time evolution of $U(1)$-invariant quantities (and thus the stability) remains the same in both frames [49].

*Method.*—To study the driven system at arbitrary frequencies, we employ a self-consistent WCCA. The WCCA involves deriving equations of motion from a two-particle irreducible effective action [50] within the nonequilibrium Schwinger-Keldysh formalism [51,52], keeping only diagrams to first order in $U$ (see [44]). Unlike simple perturbation theory or Bogoliubov theory, the WCCA respects unitarity and conservation laws [53], and thus gives physically sensible results for all times; in particular, it allows the exponential growth of unstable modes to be cut off by the resulting depletion of the condensate. While the WCCA is *not* guaranteed to yield a gapless excitation spectrum [53,54], the low-frequency behavior of the spectrum is irrelevant for the phenomena discussed here. Our approach is equivalent to a fully self-consistent, time-dependent Hartree-Fock-Bogoliubov approximation [54,55]; our formulation, however, can more readily be extended to higher orders in $U$.

The WCCA equations of motion [44] were solved numerically. For the results presented here, we prepared the system on a $N_s = 100 \times 100$ lattice in the ground state of Bogoliubov theory. We allow for a macroscopic population of the $\mathbf{k} = \boldsymbol{\pi}$ mode to allow for a condensate at momentum $\boldsymbol{\pi}$. To study the nonequilibrium dynamics, we abruptly turn on the periodic drive and propagate the initial state for 801 driving cycles using Eqs. (15) and (16) of [44]. We checked that the results are insensitive to system size.

*Stability diagram.*—The stability phase diagram is shown in Fig. 1. Previous work has investigated the driven Bose-Hubbard model [56–63] and related models [64–72] using various approximation schemes; we go beyond these works by treating both the condensate and quasiparticle sectors, including the feedback between them. Thus, we are able to explore instabilities originating in either sector on equal footing.

We first discuss two analytically tractable limits, corresponding to high-frequency driving (i.e., going along the $x$ axis of Fig. 1) and to low-amplitude driving (i.e., going along the $y$ axis). In the first case, the dynamics is approximately governed by an effective time-average Hamiltonian [5,6],

$$H_{\mathrm{ave}} = -J_{\mathrm{ave}}(\zeta) \sum_{\langle ij \rangle} b_i^\dagger b_j + \frac{U}{2} \sum_j n_j(n_j - 1). \tag{3}$$

The periodic modulation renormalizes the hopping to $J_{\mathrm{ave}}(\zeta) = J_0 \mathcal{J}_0(\zeta)$, where $\mathcal{J}_0(\zeta)$ is the zeroth-order Bessel function of the first kind, which is a damped oscillatory function with the first zero at $\zeta \approx 2.4$, the second at $\zeta \approx 5.5$, etc. Thus, as $\zeta$ is increased, the time-averaged hopping decreases, until the dispersion flattens at $\zeta \approx 2.4$. For $\zeta > 2.4$ the dispersion flips sign, and acquires a stable minimum at $\boldsymbol{\pi} = (\pi, \pi)$. Thus, in the high-frequency limit the condensate at $\mathbf{0} = (0, 0)$ is stable when $\zeta < 2.4$, whereas the condensate at $\boldsymbol{\pi}$ is stable when $2.4 \lesssim \zeta \lesssim 5.5$. Moreover, for commensurate filling, the superfluid phase should transition into a Mott insulating state around $\zeta = 2.4$ determined by the phase boundary $J_{\mathrm{ave}}(\zeta)/U \lesssim 0.06$ [73,74]. This transition regime, marked by the thin vertical strip in Fig. 1, is beyond the validity of the WCCA; our WCCA simulations in this regime give oscillatory behavior, see [44].

A second analytically tractable limit is that of weak driving, at arbitrary $\Omega$. The dominant effects can be inferred from linear stability analysis around the nondriven state. In terms of Bogoliubov quasiparticle operators $\gamma_{\mathbf{k}}$, the system-drive coupling includes terms of the form $e^{i\Omega t}\gamma_{\mathbf{k}}^\dagger \gamma_{-\mathbf{k}}^\dagger$, involving the emission of pairs of quasiparticles from the condensate. The emission rate is related to the density of states of two-quasiparticle excitations at $\Omega$. Specifically, if the nondriven system has quasiparticle excitations at energy $E_{\mathbf{k}}, E_{-\mathbf{k}}$ such that $\Omega = E_{\mathbf{k}} + E_{-\mathbf{k}}$, absorption will occur and the system will be unstable. On the other hand, if $\Omega \geq 2W$, where $W \approx 2zJ_0$ is the approximate bandwidth

of Bogoliubov excitations, then absorption does not occur and the system is stable.

Combining the insights from these two limits allows us to understand the entire stability phase diagram. The drive creates pairs of renormalized Bogoliubov quasiparticles, which have an effective bandwidth $W_{\rm ave} \approx 2zJ_{\rm ave}(\zeta)$. We define $W_{\rm ave} \equiv \max_k[E_{\rm ave}(\mathbf{k})] - \min_k[E_{\rm ave}(\mathbf{k})]$ as the time-averaged Floquet-Bogoliubov bandwidth; in terms of this, the stability condition reads

$$\Omega_c > 2W_{\rm ave} \Leftrightarrow \text{stable}. \tag{4}$$

Equation (4) is consistent with our numerical results (Fig. 1). This result is unexpected—since the time-averaged Hamiltonian is valid at infinite frequency, whereas parametric resonance is a low-frequency phenomenon—but can be understood as follows. The hopping matrix element in the driven system can be expanded as $J(t) \sim J_0 \sum_n \mathcal{J}_n(\zeta) \exp(in\Omega t)$. We absorb the time-independent $n = 0$ component in the unperturbed Hamiltonian, and treat the $n = 1$ term, which oscillates at $\Omega$, perturbatively. The perturbation is small for $U \ll \Omega$, because the matrix element for creating two quasiparticles is proportional to both $\mathcal{J}_1(\zeta)$ (which need not be small) and $U$ (which is assumed to be small). We then use parametric instability analysis [44] with the renormalized dispersion, and conclude that an instability occurs when $\Omega = 2W_{\rm ave}$. When $\Omega/J_0 \gg 1$, the critical driving frequency is given by

$$\Omega_c(\zeta) = 4\sqrt{zJ_{\rm ave}(\zeta)[zJ_{\rm ave}(\zeta) + n_0 U]}. \tag{5}$$

Note that in the present case, resonant absorption occurs for drive strengths up to *twice* the single-particle bandwidth; by contrast, in noninteracting systems, no absorption occurs for $\Omega > W_{\rm ave}$. The presence of absorption at frequencies exceeding the single-particle bandwidth is generic in interacting systems.

*Condensate evolution*.—Figure 2(a) shows the evolution of the condensate fraction in various regimes: in the parametrically unstable regime (solid blue line), the condensate slowly decays; in the stable regime (dashed red line), it saturates to a prethermalized value, which is generally lower than the Bogoliubov value [since $|J_{\rm ave}(\zeta)| < |J_0|$]. The system enters a steady state with constant in time evolution when measured stroboscopically. When the initial condensate is at the band maximum (dash-dotted black line), the condensate decays rapidly. Figure 2(b) shows the decay rate as a function of drive amplitude in the parametrically unstable regime; note that the decay rate depends not only on drive strength $\zeta$, but also on $U$ and $\Omega$. Very close to the region $\zeta \sim 2.405$ (grey strip in Fig. 1), the WCCA gives strong oscillations of the particle density between the condensates at $\mathbf{0}$ and $\boldsymbol{\pi}$ (see [44]); however, as previously noted, the WCCA is not reliable here.

A natural further observable is the total energy of the system, which grows in the unstable phases and saturates in the stable phases (see [44]).

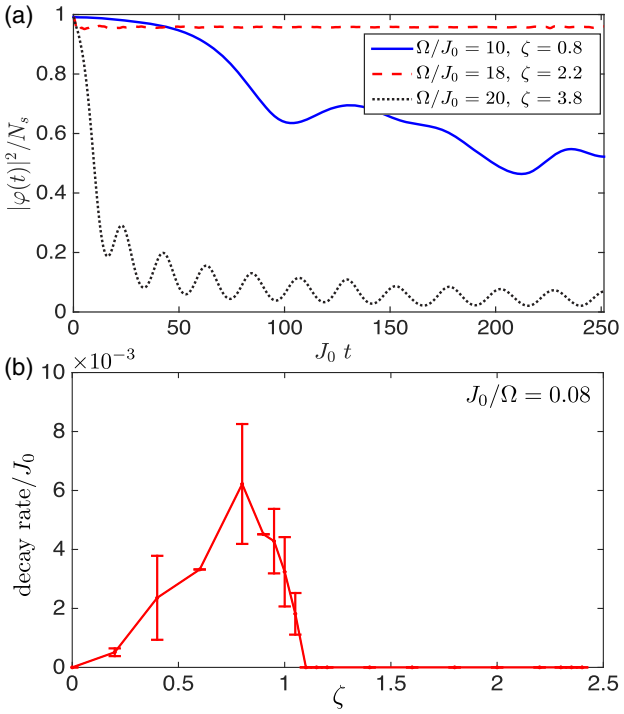


FIG. 2 (color online). (a) Time evolution of the condensate fraction for 801 driving cycles, starting from a Bogoliubov initial state localized at $\mathbf{k} = \mathbf{0}$ for $U/J_0 = 0.2$. (b) Decay rate to 75% of the condensate curves for $\Omega/J_0 = 12$ (boldface points in Fig. 1). Error bars are set by the difference of the inverse times, determined by the first and last time the curve passes through 3/4, taking into account the oscillatory behavior.

*(Quasi)momentum distribution*.—Figure 3 plots snapshots of the quasimomentum (i.e., lattice momentum) distribution; the time evolution of this quantity is shown in [44]. Specifically, the quantity plotted is $n_{\mathbf{k}} = \langle b^\dagger_{\mathbf{k}} b_{\mathbf{k}} \rangle - n_0 \delta_{k,0}$; i.e., the condensate peak is subtracted. The quasimomentum distribution can be directly accessed through band mapping followed by time-of-flight imaging. Moreover, as we are concerned with a single-band model, one can extract this distribution directly from time-of-flight imaging, by focusing on momenta within the first Brillouin zone.

Figure 3(a) shows the parametrically unstable case, where quasiparticles are strongly excited around the quasimomentum surface $\{\mathbf{k} : \Omega = 2E_{\rm ave}(\mathbf{k})\}$ matching the resonance condition. Within Bogoliubov theory, the (time-averaged) excitation intensity should be uniform along this surface. However, as the points along this surface are not symmetry related, the nonlinearities included in the WCCA favor some points on the excitation surface, as seen in the intensity pattern in Fig. 3(a).

Figure 3(b) shows the stable case. Here, by contrast with Fig. 3(a), the quasiparticle population remains low throughout the Brillouin zone. As expected from Bogoliubov theory, bosonic modes satisfying $J_{\rm ave}(\mathbf{k}) \lesssim U$ should have appreciable occupation in the steady state; this region expands as the dispersion flattens. The intricate patterns

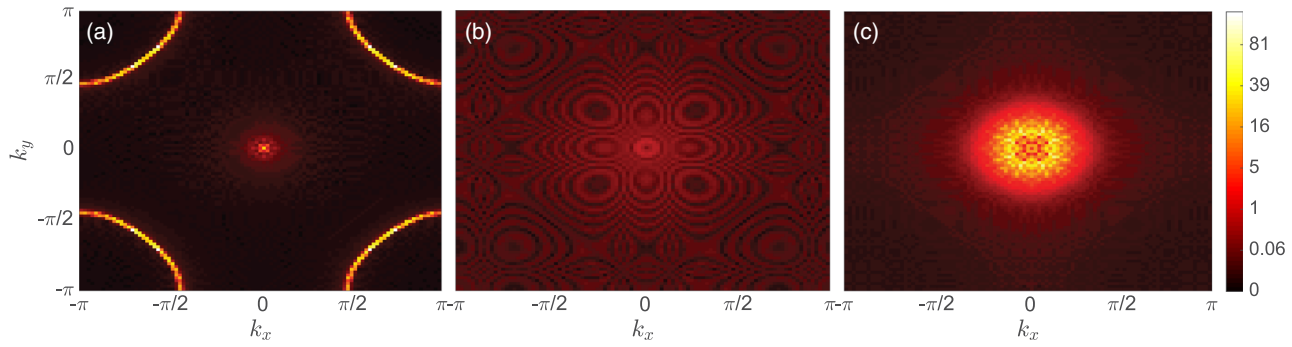


FIG. 3 (color online). Snapshot of the momentum distribution $n_{\mathbf{k}} = \langle b^{\dagger}_{\mathbf{k}} b_{\mathbf{k}} \rangle - n_0 \delta_{k,0}$ after 801 driving cycles starting from a Bogoliubov initial state localized at $\mathbf{k} = \mathbf{0}$ for $U/J_0 = 0.2$. Panel (a) is in the unstable regime where the condensate is depleted due to parametric resonance. The bosons are excited by the drive to the quasienergy surface $\Omega = 2E_{\mathrm{ave}}(\mathbf{k})$ (bright yellow-white circle around $\mathbf{k} = \boldsymbol{\pi}$) where they occupy sharp peaks (white pixels). Panel (b) is in the regime where the condensate is stable on the prethermal time scales. In panel (c), the system is dynamically unstable due to the dispersion being inverted. The bright disc of excitations around $\mathbf{k} = \mathbf{0}$ corresponds to dynamically unstable modes. The parameters are (a) $\Omega/J_0 = 10$, $\zeta = 0.8$, (b) $\Omega/J_0 = 18$, $\zeta = 2.2$, and (c) $\Omega/J_0 = 20$, $\zeta = 3.8$.

in momentum space are due to the abrupt turn-on of the drive—which initializes the Floquet-Bogoliubov quasiparticle states out of equilibrium—and are absent when the drive is instead gradually ramped up. These patterns evolve nontrivially with time (see [44]).

Finally, Fig. 3(c) illustrates the case in which the initial state is a condensate at $\mathbf{k} = \mathbf{0}$, but the dispersion is inverted ($\zeta > 2.4$) so that the only stable condensate is supported at $\mathbf{k} = \boldsymbol{\pi}$. Thus the initial state is unstable regardless of $\Omega$. Let us consider the infinite-frequency limit, which amounts to a sudden quench of the single-particle dispersion. Computing the Bogoliubov spectrum around a condensate at $\mathbf{k} = \mathbf{0}$ in an inverted dispersion, we find that modes with momenta near $\mathbf{k} = \mathbf{0}$ acquire imaginary frequencies (and thus grow exponentially), whereas modes with large momenta are stable [75]. The unstable modes are determined by the condition $\varepsilon_{\mathrm{ave}}(\mathbf{k}) + zJ_0 < 2n_0U$, where $\varepsilon_{\mathrm{ave}}(\mathbf{k})$ is the single-particle Floquet dispersion (3). These modes are dynamically stabilized due to the nonlinear feedback of the self-consistent treatment [52]. Our numerical results with the WCCA confirm this picture: the unstable modes at small quasimomenta acquire large populations, whereas the large-quasimomentum modes do not. This behavior is specific to the WCCA; in a real system it will correspond to intermediate-time dynamics $t \lesssim J_0/U^2$. On longer times, collisions between quasiparticles should cause large occupation numbers across the Brillouin zone, see [44].

*Discussion.*—We briefly outline the validity of the WCCA in the three regimes of interest (for details see [44]). In the parametrically unstable regime, the stability analysis suggests that unstable modes grow at the rate $\Gamma \sim Un_0J_0\mathcal{J}_1(\zeta)/W_{\mathrm{ave}}$, while the momentum arcs in Fig. 2(a) decay at a golden rule rate $\sim U^2n_0n_{\mathbf{k}}/W_{\mathrm{ave}}$. Hence, as long as $Un_{\mathbf{k}} < J_0\mathcal{J}_1(\zeta)$, the formation rate is greater than the decay rate and the WCCA is reliable. In the stable region, the condensate fraction $n_0$ remains large, and the WCCA remains valid until very late times, when resonant absorption involving $m = \Omega/W_{\mathrm{ave}}$ quasiparticles becomes dominant. For large $\Omega$, this is a very high-order and, therefore, very slow process. Finally, in the dynamically unstable phase, the WCCA physics is valid up to times $W_{\mathrm{ave}}/U^2$ (the collisional time scale). Thus, at weak coupling, there is a parametrically large window between $1/\sqrt{J_{\mathrm{ave}}(\zeta)U}$ and $W_{\mathrm{ave}}/U^2$ where the WCCA description is correct.

The main experimental prediction of this Letter—a parametric change in heating rates as a function of drive amplitude and frequency—can be measured in present-day experiments, which are naturally in the weak-coupling regime. For the experiment in Ref. [26] the parameters were chosen as $U/J_0 \approx 0.1$, $\Omega/J_0 \approx 20$, and $\zeta \approx 0.6$, which is within the regime we considered. For realistic experiments in optical lattices, the presence of higher bands can lead to instability even at high drive frequencies $\Omega$. In this case there are three regimes: (i) if $\Omega$ is less than twice the renormalized bandwidth $W_{\mathrm{ave}}$ of the lower band, the system is parametrically unstable as discussed above; (ii) if $\Omega$ is larger than $2W_{\mathrm{ave}}$, smaller than the band gap to the upper band, and furthermore chosen such that any $n$-photon resonances to higher bands [76] are suppressed, then the system is stable within WCCA; (iii) if $\Omega$ exceeds the band gap, the drive can mediate interband transitions, leading to instability again. For a square optical lattice with typical lattice potential $V_{\mathrm{latt}} = 10E_{\mathrm{recoil}}$, $E_{\mathrm{recoil}} = h \times 4$ kHz, the bandwidth of the lowest band is $W_0 = 4J_0 = h \times 0.3$ kHz [the time-averaged bandwidth $W_{\mathrm{ave}}$ is reduced by a factor of $\mathcal{J}_0(\zeta)$], and the gap to the second Bloch band is $\Delta = 4.57E_{\mathrm{recoil}} = h \times 18.28$ kHz.

Although we focused on a square lattice, the arguments generalize to other lattices, such as the honeycomb lattice, in which topologically nontrivial states exist. Note that topological gaps in mechanically shaken optical lattices scale as $\Omega^{-1}$ [23–25]. Hence, in order to engineer topological insulators with large gaps (and a large region of nonzero Berry curvature around them), it is desirable to go to lower frequencies. Our results impose a fundamental limit for weakly interacting bosonic systems on how small the

frequency can be, since for $\Omega < 2W_{\mathrm{ave}}$ the system becomes unstable. More generally, our results suggest that conserving approximations, whether controlled by weak coupling or some other parameter as in large-$N$ models [52,77–80], are ways of exploring dynamical phase transitions in models that are both interacting (unlike free-particle models) and finite-dimensional (unlike the Kapitza pendulum). The critical properties of such transitions are a fruitful theme for future work. Although in practice such phase transitions will be smeared out by higher-order effects, the associated crossovers should still be experimentally observable.

We thank D. Abanin, M. Babadi, I. Bloch, L. D'Alessio, E. Dalla Torre, N. Goldman, M. Kolodrubetz, A. Polkovnikov, and U. Schneider for interesting and fruitful discussions, and we especially acknowledge the help of M. Lohse in determining the experimentally relevant parameters. The authors acknowledge support from the NSF Grant No. DMR-1308435, Harvard-MIT CUA, AFOSR New Quantum Phases of Matter MURI, the ARO-MURI on Atomtronics, ARO MURI Quism program, AFOSR Grant No. FA9550-13-1-0039 and BSF Grant No. 2010318, and Technical University Munich—Institute for Advanced Study, funded by the German Excellence Initiative and the European Union FP7 under Grant No. 291763.

*mbukov@bu.edu

[1] J. H. Shirley, Phys. Rev. **138**, B979 (1965).
[2] H. Sambe, Phys. Rev. A **7**, 2203 (1973).
[3] H. P. Breuer, K. Dietz, and M. Holthaus, Physica (Amsterdam) **46D**, 317 (1990).
[4] H. P. Breuer and M. Holthaus, Ann. Phys. (N.Y.) **211**, 249 (1991).
[5] N. Goldman and J. Dalibard, Phys. Rev. X **4**, 031027 (2014).
[6] M. Bukov, L. D'Alessio, and A. Polkovnikov, Adv. Phys. **64**, 139 (2015).
[7] A. Eckardt and E. Anisimovas, New J. Phys. **17**, 093039 (2015).
[8] D. H. Dunlap and V. M. Kenkre, Phys. Rev. B **34**, 3625 (1986); Phys. Rev. B **37**, 6622 (1988).
[9] A. Eckardt, C. Weiss, and M. Holthaus, Phys. Rev. Lett. **95**, 260404 (2005).
[10] H. Lignier, C. Sias, D. Ciampini, Y. Singh, A. Zenesini, O. Morsch, and E. Arimondo, Phys. Rev. Lett. **99**, 220403 (2007).
[11] A. Zenesini, H. Lignier, D. Ciampini, O. Morsch, and E. Arimondo, Phys. Rev. Lett. **102**, 100403 (2009).
[12] C. E. Creffield, F. Sols, D. Ciampini, O. Morsch, and E. Arimondo, Phys. Rev. A **82**, 035601 (2010).
[13] G. Jotzu, M. Messer, F. Görg, D. Greif, R. Desbuquois, and T. Esslinger, Phys. Rev. Lett. **115**, 073002 (2015).
[14] J. Struck, C. Ölschläger, R. Le Targatn, P. Soltan- Panahi, A. Eckardt, M. Lewenstein, P. Windpassinger, and K. Sengstock, Science **333**, 996 (2011).
[15] D. Jaksch and P. Zoller, Ann. Phys. (Amsterdam) **315**, 52 (2005).
[16] E. J. Mueller, Phys. Rev. A **70**, 041603 (2004).
[17] J. Struck, M. Weinberg, C. Ölschläger, P. Windpassinger, J. Simonet, K. Sengstock, R. Höppner, P. Hauke, A. Eckardt, M. Lewenstein, and L. Mathey, Nat. Phys. **9**, 738 (2013).
[18] M. Aidelsburger, M. Atala, M. Lohse, J. T. Barreiro, B. Paredes, and I. Bloch, Phys. Rev. Lett. **111**, 185301 (2013).
[19] H. Miyake, G. A. Siviloglou, C. J. Kennedy, W. C. Burton, and W. Ketterle, Phys. Rev. Lett. **111**, 185302 (2013).
[20] M. Atala, M. Aidelsburger, M. Lohse, J. T. Barreiro, B. Paredes, and I. Bloch, Nat. Phys. **10**, 588 (2014).
[21] C. J. Kennedy, W. C. Burton, W. Ch. Chung, and W. Ketterle, Nat. Phys. **11**, 859 (2015).
[22] N. Fläschner, B. S. Rem, M. Tarnowski, D. Vogel, D.-S. Lühmann, K. Sengstock, and C. Weitenberg, arXiv:1509.05763.
[23] T. Oka and H. Aoki, Phys. Rev. B **79**, 081406(R) (2009).
[24] T. Kitagawa, T. Oka, A. Brataas, L. Fu, and E. Demler, Phys. Rev. B **84**, 235108 (2011).
[25] G. Jotzu, M. Messer, R. Desbuquois, M. Lebrat, T. Uehlinger, D. Greif, and T. Esslinger, Nature (London) **515**, 237 (2014).
[26] M. Aidelsburger, M. Lohse, C. Schweizer, M. Atala, J. T. Barreiro, S. Nascimbène, N. R. Cooper, I. Bloch, and N. Goldman, Nat. Phys. **11**, 162 (2015).
[27] N. H. Lindner, G. Refael, and V. Galitski, Nat. Phys. **7**, 490 (2011).
[28] M. S. Rudner, N. H. Lindner, E. Berg, and M. Levin, Phys. Rev. X **3**, 031005 (2013).
[29] M. Bukov, M. Kolodrubetz, and A. Polkovnikov, arXiv:1510.02744.
[30] J. M. Deutsch, Phys. Rev. A **43**, 2046 (1991).
[31] M. Srednicki, Phys. Rev. E **50**, 888 (1994).
[32] M. Rigol, V. Dunjko, and M. Olshanii, Nature (London) **452**, 854 (2008).
[33] L. D'Alessio and A. Polkovnikov, Ann. Phys. (Amsterdam) **333**, 19 (2013).
[34] L. D'Alessio and M. Rigol, Phys. Rev. X **4**, 041048 (2014).
[35] A. Lazarides, A. Das, and R. Moessner, Phys. Rev. Lett. **112**, 150401 (2014).
[36] A. Lazarides, A. Das, and R. Moessner, Phys. Rev. E **90**, 012110 (2014).
[37] P. Ponte, Z. Papić, F. Huveneers, and D. A. Abanin, Phys. Rev. Lett. **114**, 140401 (2015).
[38] D. Abanin, W. De Roeck, and F. Huveneers, arXiv:1507.01474.
[39] T. Kuwahara, T. Mori, and K. Saito, arXiv:1508.05797.
[40] T. Mori, T. Kuwahara, and K. Saito, arXiv:1509.03968.
[41] D. A. Abanin, W. De Roeck, and W. W. Ho, arXiv:1510.03405.
[42] J. Berges, S. Borsanyi, and C. Wetterich, Phys. Rev. Lett. **93**, 142002 (2004).
[43] E. Canovi, M. Kollar, and M. Eckstein, arXiv:1507.00991.
[44] See Supplemental Material at http://link.aps.org/supplemental/10.1103/PhysRevLett.115.205301, which includes Refs. [45–48], for important information used to arrive at the results and conclusions of the main text. In particular, we provide a derivation of the WCCA equations of motion for a general bipartite lattice, and discuss the validity of the WCCA when collisions are taken into account. Furthermore, a detailed instability analysis is

presented within Bogoliubov theory. The time-dependence of the total energy is shown in the parametrically unstable, the stable and the dynamically unstable regimes. Finally, we also discuss the time dependence of the momentum distribution function, and provide three videos to illustrate it.
[45] M. Bukov and M. Heyl, Phys. Rev. B **86**, 054304 (2012).
[46] L. D. Landau and E. M. Lifshitz, *Mechanics* (Elsevier, Amsterdam, 2008).
[47] A. Kamenev, *Field Theory of Non-Equilibrium Systems* (Cambridge University Press, Cambridge, England, 2011).
[48] M. Greiner, O. Mandel, T. W. Hänsch, and I. Bloch, Nature (London) **419**, 51 (2002).
[49] M. Bukov and A. Polkovnikov, Phys. Rev. A **90**, 043613 (2014).
[50] J. M. Cornwall, R. Jackiw, and E. Tomboulis, Phys. Rev. D **10**, 2428 (1974).
[51] J. Bauer, M. Babadi, and E. Demler, Phys. Rev. B **92**, 024305 (2015).
[52] M. Babadi, E. Demler, and M. Knap, Phys. Rev. X **5**, 041005 (2015).
[53] P. C. Hohenberg and P. C. Martin, Ann. Phys. (N.Y.) **34**, 291 (1965).
[54] A. Griffin, Phys. Rev. B **53**, 9341 (1996).
[55] A. M. Rey, B. L. Hu, E. Calzetta, A. Roura, and C. W. Clark, Phys. Rev. A **69**, 033610 (2004).
[56] A. Buchleitner and A. R. Kolovsky, Phys. Rev. Lett. **91**, 253002 (2003).
[57] A. R. Kolovsky and A. Buchleitner, Phys. Rev. E **68**, 056213 (2003).
[58] A. Tomadin, R. Mannella, and S. Wimberger, Phys. Rev. Lett. **98**, 130402 (2007).
[59] A. R. Kolovsky, H. J. Korsch, and E.-M. Graefe, Phys. Rev. A **80**, 023617 (2009).
[60] C. E. Creffield, Phys. Rev. A **79**, 063612 (2009).
[61] A. Kolovsky, Europhys. Lett. **93**, 20003 (2011); C. E. Creffield and F. Sols, Europhys. Lett. **101**, 40001 (2013).
[62] C. A. Parra-Murillo, J. Madroñero, and S. Wimberger, Phys. Rev. A **88**, 032119 (2013).
[63] C. A. Parra-Murillo, J. Madroñero, and S. Wimberger, Comput. Phys. Commun. **186**, 19 (2015).
[64] T. Stöferle, H. Moritz, C. Schori, M. Köhl, and T. Esslinger, Phys. Rev. Lett. **92**, 130403 (2004).
[65] C. Schori, T. Stöferle, H. Moritz, M. Köhl, and T. Esslinger, Phys. Rev. Lett. **93**, 240402 (2004).
[66] M. Krämer, C. Tozzo, and F. Dalfovo, Phys. Rev. A **71**, 061602(R) (2005).
[67] C. Tozzo, M. Krämer, and F. Dalfovo, Phys. Rev. A **72**, 023613 (2005).
[68] I. Carusotto, R. Balbinot, A. Fabbri, and A. Recati, Eur. Phys. J. D **56**, 391 (2009).
[69] C. Zhang, J. Liu, M. G. Raizen, and Q. Niu, Phys. Rev. Lett. **92**, 054101 (2004).
[70] S. Choudhury and E. J. Mueller, Phys. Rev. A **91**, 023624 (2015).
[71] T. Bilitewski and N. R. Cooper, Phys. Rev. A **91**, 063611 (2015).
[72] S. Choudhury and E. J. Mueller, arXiv:1508.07572.
[73] B. Capogrosso-Sansone, S. G. Soyler, N. Prokofev, and B. Svistunov, Phys. Rev. A **77**, 015602 (2008).
[74] M. Knap, E. Arrigoni, and W. von der Linden, Phys. Rev. B **81**, 024301 (2010).
[75] This might seem counterintuitive, as the larger-momentum modes have "more negative" energies; note, however, that in the $U \to 0$ limit, *all* modes are stable as there are no decay processes.
[76] M. Weinberg, C. Ölschlger, C. Sträter, S. Prelle, A. Eckardt, K. Sengstock, and J. Simonet, arXiv:1505.02657 [Phys. Rev. Lett. (to be published)].
[77] M. Moshe and J. Zinn-Justin, Phys. Rep. **385**, 69 (2003).
[78] B. Sciolla and G. Biroli, Phys. Rev. B **88**, 201110(R) (2013).
[79] P. Smacchia, M. Knap, E. Demler, and A. Silva, Phys. Rev. B **91**, 205136 (2015).
[80] A. Chandran and S. L. Sondhi, arXiv:1506.08836.